International Scholarly Research Network
ISRN Anesthesiology
Volume 2012, Article ID 261640, 11 pages
doi:10.5402/2012/261640

Research Article

MicroPET/CT Imaging of [^{18}F]-FEPPA in the Nonhuman Primate: A Potential Biomarker of Pathogenic Processes Associated with Anesthetic-Induced Neurotoxicity

Xuan Zhang,[1] Merle G. Paule,[1] Glenn D. Newport,[1] Fang Liu,[1] Ralph Callicott,[1] Shuliang Liu,[1] Marc S. Berridge,[2,3] Scott M. Apana,[2,3] William Slikker Jr.,[1] and Cheng Wang[1]

[1] *National Center for Toxicological Research, US Food and Drug Administration, Jefferson, AR 72079, USA*
[2] *3D Imaging, LLC, Little Rock, AR 72113, USA*
[3] *University of Arkansas for Medical Sciences, Little Rock, AR 72205, USA*

Correspondence should be addressed to Cheng Wang, cheng.wang@fda.hhs.gov

Received 6 August 2012; Accepted 15 September 2012

Academic Editors: J. Abraini and J.-H. Baumert

Background. The inhalation anesthetics nitrous oxide (N_2O) and isoflurane (ISO) are used in surgical procedures for human infants. Injury to the central nervous system is often accompanied by localization of activated microglia or astrocytosis at the site of injury. The tracer that targets to the peripheral benzodiazepine receptor (PBR), [^{18}F]N-2-(2-fluoroethoxy)benzyl)-N-(4-phenoxypyridin-3-yl)acetamide ([^{18}F]-FEPPA), has been reported as a sensitive biomarker for the detection of neuronal damage/inflammation. *Methods*. On postnatal day (PND) 5 or 6 rhesus monkey neonates were exposed to a mixture of N_2O/oxygen and ISO for 8 hours and control monkeys were exposed to room air. MicroPET/CT images with [^{18}F]-FEPPA were obtained for each monkey 1 day, one week, three weeks, and 6 months after the anesthetic exposure. *Results*. The radiotracer quickly distributed into the brains of both treated and control monkeys on all scan days. One day after anesthetic exposure, the uptake of [^{18}F]-FEPPA was significantly increased in the temporal lobe. One week after exposure, the uptake of [^{18}F]-FEPPA in the frontal lobe of treated animals was significantly greater than that in controls. *Conclusions*. These findings suggest that microPET imaging is capable of dynamic detection of inhaled anesthetic-induced brain damage in different brain regions of the nonhuman primate.

1. Introduction

General anesthetics bring about a reversible loss of consciousness by regulating neuronal excitability. The mechanisms underlying this action include suppression of excitatory NMDA receptor-mediated transmission and/or potentiation of inhibitory $GABA_A$ receptor currents in the central nervous system [1–3]. Nitrous oxide (N_2O), a gaseous inhalation anesthetic agent, is often given in combination with more powerful volatile anesthetics such as isoflurane (ISO) to maintain general anesthesia in pregnant women, neonates and infants requiring surgery and/or other invasive or painful procedures.

Experimental findings both in vitro and in vivo suggest that general anesthetics can induce neurotoxicity during the period of rapid neuronal growth and synaptogenesis (the brain growth spurt period) in the developing animal brain [1, 4–6]. Because of the similarity of the physiology, pharmacology, metabolism, reproductive systems, and developmental trajectory and time course of the nonhuman primate to that of the human, they are exceptionally good animal models of neurodevelopment and for the detection of potential neurodegenerative effects associated with exposure to inhaled anesthetics. In a parallel study [7], a combination of 70% N_2O + 1% ISO was also utilized to achieve and maintain a surgical plane of anesthesia. Neonatal rhesus monkeys were exposed on PND 5 or 6 to N_2O plus ISO for 8 hours and 6 hours after termination of the exposure the brains were fixed and subsequently examined for neurotoxic effects. Significantly elevated neuronal damage, as indicated by increased numbers of caspase-3-, silver stain-, and Fluoro-Jade C-positive cells, was observed in neocortical areas,

especially in layers II and III of the frontal cortex, temporal gyrus and hippocampus.

These observations have heightened concerns about whether such effects are temporary (lasting only a few days after exposure) or long-term (lasting weeks or months) in infants and children undergoing inhaled anesthetic-induced anesthesia. Additionally, recent epidemiological studies have demonstrated a relationship between anesthesia and surgery in childhood and later development of behavioral abnormalities and learning disabilities [8–11]. Thus, to further study the long-term CNS effects that occur in association with inhaled anesthetic-induced anesthesia, the development of tools for the minimally invasive imaging of relevant neuronal damage is highly desirable.

Molecular imaging using positron emission tomography (PET) is a leading modality for obtaining non- or minimally invasive in vivo measurements of multiple biological processes in various organs. The development of microPET imaging applications has provided the ability to collect sensitive and quantitative three-dimensional molecular information from the living brains of a variety of animals including nonhuman primates (NHP) [12–14]. In order to obtain sufficient data from living animals and longitudinally assess the neurotoxic effects associated with developmental exposures to anesthesia, we have developed a microPET protocol thought to target neuronal damage in vivo using imaging approaches [15, 16]. Since levels of the peripheral benzodiazepine receptor (PBR) are thought to increase in areas of neuronal injury following exposure to neurotoxicants [17], the PBR is widely recognized as an important target for imaging via PET [17–19]. In this study, [^{18}F]-radiolabelled]-N-(2-(2-fluoroethoxy)benzyl)-N-(4-phenoxypyridin-3-yl) acetamide)([^{18}F]-FEPPA) was utilized as an imaging agent for PBRs in the central nervous system of neonatal monkeys.

2. Materials and Methods

2.1. Animals. All animal procedures were approved by the National Center for Toxicological Research (NCTR) Institutional Animal Care and Use Committee and conducted in full accordance with the PHS Policy on Humane Care and Use of Laboratory Animals.

All monkeys were born and housed at the FDA's National Center for Toxicological Research nonhuman primate research facility. Animal procedures were designed to minimize the number of animals required and any pain or distress associated with the experimental procedures.

A total of eight (PND 5 or 6, 460–500 g) rhesus monkeys (*Macaca mulatta*) were utilized. Three male and five female monkeys were randomly assigned to treatment ($n = 4$, 1 male, 3 females) and control ($n = 4$, 2 males, 2 females) groups. Immediately prior to the initiation of anesthesia or sequestration, the neonates were separated from their anesthetized mothers, removed from their home cage and hand carried to a procedure room. Control animals were maintained in a holding cage other than the exposure chamber with water, but no food, and were not sedated for physiological measurements or blood sample collections. Animals in the treated group were exposed to a mixture of 70% N_2O/30% oxygen and 1% ISO for 8 hours.

2.2. Experimental Procedures. Nitrous oxide (N_2O) and oxygen were delivered using a calibrated anesthetic machine with blender (Bird Corporation, Palm Springs, CA, USA). Isoflurane (ISO) was delivered using an agent-specific vaporizer (E-Z Anesthesia, Palmer, PA, USA) attached to the anesthetic machine. To administer a specific concentration of N_2O/oxygen/ISO in a tightly controlled environment, an anesthesia chamber (Euthanex Corp. Palmer, PA, USA) was used. Monkeys were kept in this chamber with a circulating water heating pad to maintain body temperature at approximately 37°C throughout the experiment. Stable gas and volatile anesthetic concentrations were attained in the chamber within 5 min of the start of exposure. For controls, room air was used in place of the inhalation anesthetics. For the treated group, the N_2O/oxygen/ISO mixture was continuously delivered to the chamber for the duration of the 8 hour exposure. A relief valve on the anesthesia chamber allowed escape of gases to avoid accumulation of carbon dioxide and waste anesthetic gas was scavenged using an attached canister containing activated charcoal.

During the experimental period, dextrose (5%) was administered by stomach tube (5 mL) every 2 h to both treated and control monkeys to maintain blood glucose levels. Glycopyrrolate (0.01 mg/kg, American Reagent, Shirley, NY, USA) was administered intramuscularly prior to anesthesia to both treated and control monkeys to reduce airway secretions. Once exposures were complete, animals were monitored in an incubator until complete recovery and then returned to their mothers (approximately 2 hours). Control animals were kept in the exposure chambers under room air for a total of 10 hours (8 + 2).

2.3. Monitoring of Physiological Parameters. The physiological parameters of the neonatal monkeys were monitored following procedures described previously [20, 21] Briefly, noninvasive pulse oximetry (N-395 Pulse Oximeter, Nellcor, Pleasanton, CA, USA; MouseO_X Plus Vital Sign Monitor, Starr Life Sciences, Oakmont, PA, USA), capnography (Tidal Wave Hand-held capnography, Respironics, Murrysville, PA, USA), and sphygmomanometry (Critikon Dynamap Vital Signs Monitor, GE Healthcare, Waukesha, WI, USA), and a rectal temperature probe were used to verify the physiological status of subjects. Heart and respiration rates, arterial blood O_2 saturation levels, expired CO_2 concentrations, and rectal temperatures, systolic and diastolic blood pressures were recorded every one or two hours in anesthetized and control animals, respectively. Venous blood (approximately 250 μL) was collected at two-hour intervals for measurement of plasma glucose concentrations, venous blood gases, Ph values, and hematocrits (GEM Premier 4000, Instrumentation Laboratory, Lexington, MA, USA). Statistical analyses of physiological parameters were performed using Student's *t*-test for comparisons between treated and control groups. One-way analysis of variance was used to evaluate the effect

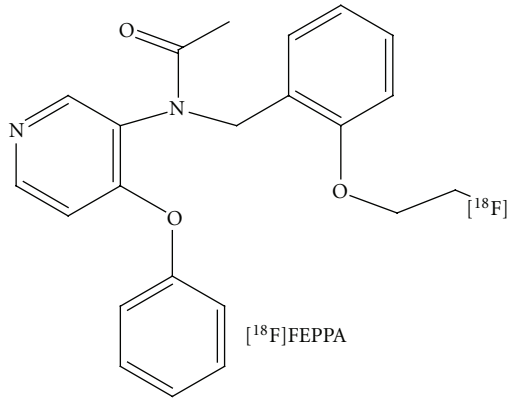

Figure 1: Chemical structure of [18F]-radiolabelled phenoxyanilide, [18F]-FEPPA.

of time under anesthesia on the body temperatures. The null hypothesis was rejected at a probability level of $P < 0.05$.

2.4. Radiotracer Preparation. [18F]-FEPPA (Figure 1) was prepared by 3D-Imaging LLC (Little Rock, AR) according to Wilson et al. [19] from the corresponding tosylate as described therein with minor modifications to the procedure. [18F]-FEPPA was produced in >98% purity at a specific activity EOS of 1.1–3.7 TBq (30–100 Ci)/μmole, as compared to the previously reported value of 11–37 MBq (0.3–1 Ci)/μmole [22]. Specific activity at the time of use was one tenth to two-thirds of the EOS value.

2.5. MicroPET. A commercial high resolution small animal PET scanner (Focus 220, Siemens Preclinical Solution, Knoxville, USA) was used to quantitatively acquire images of the monkey brain. The scanner has 96 lutetium oxyorthosilicate detectors and provides a transaxial resolution of 1.35 mm full-width at half-maximum. Data were collected in a $128 \times 128 \times 95$ matrix with a pixel width of 0.475 mm and a slice thickness of 0.815 mm.

2.6. Computed Tomography. Monkeys were also imaged in a newly developed mobile neurological CereTom CT scanner (Neurologica Corps. Danvers, MA, USA). The CT gantry of the CereTom scanner moves while the subject remains externally supported and fixed in space and therefore allows it to be physically connected to the microPET scanner. Exposure settings for each CT scan were 120 kVp, 5 mAs, scan time = 120 s. Data were collected in a 512×512 matrix with a pixel width of 0.49 mm and a slice thickness of 1.25 mm.

2.7. MicroPET/CT Image Acquisition. The first microPET and CT scans of each monkey brain were taken on PND 6 or 7, the day following the experimental exposures on PND 5 or 6. Follow-up microPET/CT scans occurred approximately one week (PND 14 or 15?), three weeks (PND 30 or 31?) and 6 months following treatment (at 6 months of age). For collection of the microPET/CT images, animals were positioned on a modified external bed controlled by the microPET unit. The bed replaced the standard microPET bed and allowed for sufficient travel to move animals through the microPET and CT fields of view (over an axial range of greater than 50 cm). Throughout microPET/CT imaging sessions, monkeys were anesthetized with 1.5% isoflurane gas alone delivered through a custom face mask, and an electronic heating pad was used to maintain body temperature at approximately 37°C. For each imaging session [18F]-FEPPA (56 MBq) was injected into the lateral saphenous vein of each animal (anesthetized). Immediately following the injection, a set of serial microPET images was collected to assess the influx of the tracer for 2 hours (24 frames, 5 min each). Microcomputed tomography (microCT) coronal images were obtained immediately after microPET imaging for the purpose of fusing anatomical (CT) with molecular (PET) data. The microCT images were acquired for 2 min and concurrent image reconstruction was achieved using 3D reconstruction software (ASIPro; Concorde Microsystems, Inc, Knoxville, TN, USA) installed in the CereTom CT controller unit. Once scanning was complete, animals were monitored in an incubator within a shielded isolation area until complete recovery and then returned to their mothers (approximately 2 hours). Control animals were kept in the exposure chambers under room air for the same amount of time.

2.8. Imaging Data Analysis. Medical image analysis software, ASIPro (Concorde Microsystems, Inc, Knoxville, TN, USA) was used for the anatomical/molecular data fusion and statistical analyses. Regions of Interest (ROIs) were outlined and measured using tools provided by ASIPro. Radioactivity in different brain areas was also quantified using this software. All images were displayed using the same color scale, shown in Figure 2. Tracer accumulations in the ROIs in the left frontal and left temporal cortex were converted to SUVs. The SUVs for the ROIs were compared between control and treatment groups at a variety of time points using RM ANOVA. All values are presented as means ± SEM A P value of less than 0.05 was considered statistically significant.

2.9. Electron Microscopy (EM). To better understand the nature of inhalation anesthetic-induced neuronal damage monkey infants (PND 5 or 6) were randomly assigned in a parallel study [7] to treatment ($n = 5$; 1 male and 4 females) and control ($n = 5$; 2 males and 3 females) groups. Six hours after exposures were terminated, brain tissues were obtained for EM observations. Samples were taken from the frontal cortex (left hemisphere) and fixed in ice-cold (4°C) 2% paraformaldehyde and 0.1% glutaraldehyde in 0.1 M phosphate buffer (pH 7.4). The tissue was washed (3×30 minutes) in 0.1 M phosphate buffer (pH 7.4), postfixed with 1% osmium tetroxide in 0.1 M cacodylate buffer, then washed with 25% and 50% ethanol plus 5% uranyl acetate, followed by dehydration in an ascending ethanol series and embedded in Epon. The semisections (1 μm) were counterstained with Toluidine Blue dye and then examined under a

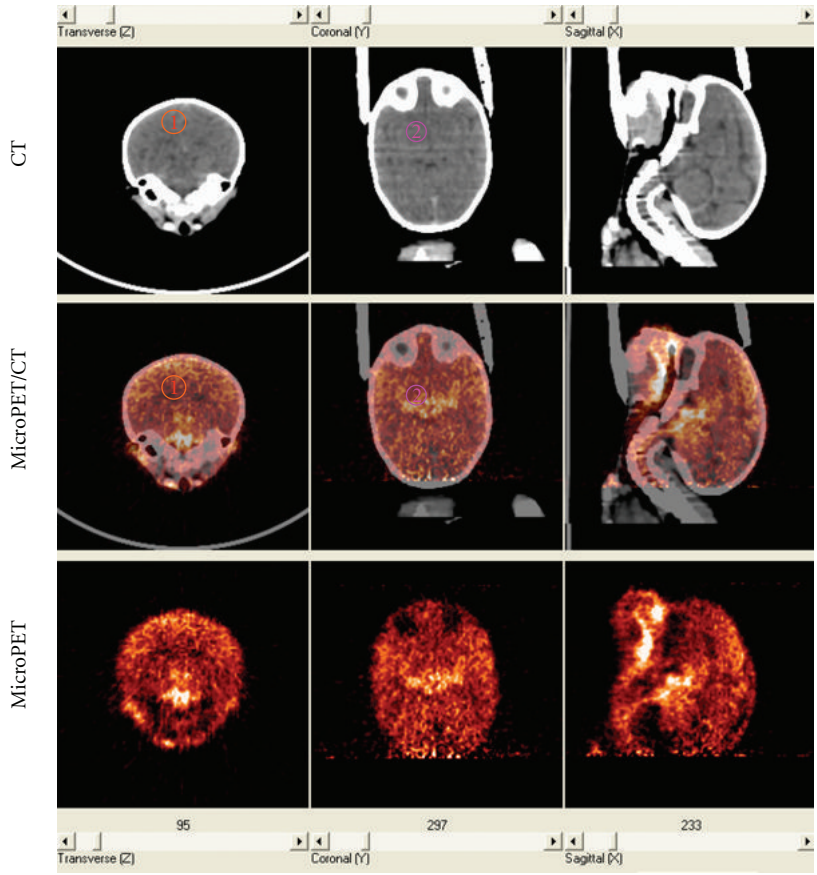

Figure 2: MicroPET and CT scans of a treated monkey brain injected with 56 MBq of [^{18}F]-FEPPA. The microPET and the CT scans began immediately and 2 h after the [^{18}F]-FEPPA injections, respectively. Top row: CT images; bottom row: microPET images; middle row: fused PET/CT images. 1: ROI is in left frontal cortex; 2: ROI is in left temporal cortex.

Nikon light microscope. The thin sections were then counterstained with uranyl acetate and lead citrate, and randomly selected fields were examined at 60 kV using a Philips CM100 electron microscope.

3. Results

3.1. Physiological Responses to Inhaled Anesthetic Agents. All the monkeys tolerated the procedures well and recovered from the anesthesia or sequestration readily and were returned to and accepted by their mothers without incident. During the exposure to the combination of 70% nitrous oxide plus 1% isoflurane, some of the physiological parameters of treated monkeys were attenuated in comparison with controls. Nevertheless, all values for the cardinal physiological parameters including blood O_2 saturation level, body temperature, and blood glucose remained within normal ranges for both treated and control monkeys [20]. Generally, these data suggested that, in agreement with a previous study [7], the inhalational anesthetics induced-neurotoxicity is not associated with adverse physiological conditions including hypothermia, hypoxia, or hypoglycemia. The physiological parameters for both groups are summarized in Table 1. Respiratory and heart rates declined slightly in the treated monkeys; however, the expired CO_2 values (mmHg) remained similar to those of control subjects. While the body temperatures of treated animals were lower than those of the controls, they were maintained above 90°F and did not decrease as the time under anesthesia increased ($P > 0.05$, One-way ANOVA).

3.2. Coregistration of MicroPET Images with CT Images for Anatomical Localization. Coronal CT images were obtained immediately after the microPET scans for the purpose of anatomical/molecular data fusion. Figure 2 represents the microPET/CT brain images from an exposed monkey: the PET/CT images were fused using ASIPro software. Using the Fusion Tool in the ASIPro software, multiple data sets (anatomical and functional) can be loaded in the same general orientation and viewed using either linked or fused views. As shown in Figure 2, the anatomical (CT) images are displayed in the top row and the functional (microPET) images in the bottom row. Once the images were loaded, the anatomical images were transposed onto the functional images and "fused" images were created, as seen in the middle row.

Table 1: Physiological parameters[#] for baby monkeys in control and treated groups.

	Control ($n = 4$)	70% N_2O + 1% isoflurane ($n = 5$)
Respiratory rate (breaths per min)	74.1 ± 18.7	66.5 ± 20.3
Expired CO_2 (mm Hg)	14.4 ± 3.3	14.5 ± 2.4
Heart Rate (beats per min)	194.4 ± 69.2	163.5 ± 30.2*
O_2 saturation (%)	95.2 ± 2.7	97.5 ± 2.4**
Body temperature (°F)	99.2 ± 2.1	92.5 ± 1.9**
Systolic blood pressure (mmHg)	97.2 ± 21	105.5 ± 30.2
Diastolic blood pressure (mmHg)	78.6 ± 18.7	82.7 ± 26.1
Glucose (mg/dL)	54.5 ± 13.2	62.4 ± 16.6
Venous pH	7.28 ± 0.07	7.24 ± 0.08
Hematocrit (%)	45.6 ± 6.4	42.4 ± 11.8

[#]The values are presented as means ± standard deviations across all time points. * and ** denote statistically significant differences between control and exposed groups with $P < 0.05$ or $P < 0.01$, respectively.

3.3. Dynamic [^{18}F]-FEPPA Uptake in the Cerebral Cortex. After the first microPET/CT scans were taken on PND 6 or 7, follow-up scans were obtained for each monkey on PNDs 14 and 30 and at 6-months of age. For each microPET scan, images were obtained over 2 hours following the injection of [^{18}F]-FEPPA and time activity curves (TACs) from the frontal and temporal cortices (the most vulnerable brain areas) [6, 7] were obtained. Tracer accumulations in the ROIs were converted to SUVs. [^{18}F]-FEPPA was observed in ROIs in both control and treated animals demonstrating that it was capable of accessing these brain areas. Examples of the first microPET scans (24 hours after exposure) are shown in Figure 3 as coronal images highlighting [^{18}F]-FEPPA brain concentrations in a control (Figure 3(a)) and treated (Figure 3(b)) monkey. The accumulation of [^{18}F]-FEPPA was clearly increased in cortical areas such as the temporal lobe, with significant differences being observed at some time points (Figure 3(c)). The uptake of [^{18}F]-FEPPA in the frontal lobe of treated animals was not significantly increased even though SUVs at most time points were higher than in controls.

On PND14, approximately one week after the anesthetic exposure, SUVs in both the frontal and temporal cortical areas were higher in the exposed animals than in the controls at all time points, demonstrating an increased uptake and retention of [^{18}F]-FEPPA in treated subjects (Figure 4). Significant differences, however, occurred only in the frontal cortical area.

On PND 30, about 3 weeks after anesthetic exposure, the uptake of [^{18}F]-FEPPA in the anesthetic-exposed monkeys tended to be higher than that in the controls at most of the time points, although no significant differences were observed at any time (Figure 5).

At the age of 6 months, the uptake of [^{18}F]-FEPPA in the anesthetic-exposed monkeys was similar to that of controls at most of the time points and no significant differences were observed at any time.

3.4. Assessment of Inhaled Anesthetic-Induced Neurotoxicity. Inhaled anesthetic-induced neurotoxicity was examined at the electron microscope (EM) level and direct evidence of increased neuronal damage after inhaled anesthetic exposure in infant monkeys was confirmed. Figure 6(a) shows a representative cortical pyramidal neuron from the frontal cortex of a control animal with intact cytoplasm and nuclear membrane. In contrast, inhalation of the combined anesthetics was associated with frontal cortical neurons that were characterized by the typical nuclear condensation thought to represent advanced stages of apoptosis (Figure 6(b)) and by morphological changes associated with necrosis (Figure 6(b)) including swelling of the mitochondria and cell body.

4. Discussion

The peripheral benzodiazepine receptor (PBR), also known as translocator protein (18 kDa) (TPSO), was first identified in 1977 and subsequently distinguished from the central benzodiazepine receptor (CBR) structurally, functionally, physiologically and pharmacologically [23, 24]. The main functions of the PBR include: cholesterol binding and transport essential for biosynthesis of steroids and bile salts; protein import for biogenesis of membranes; porphyrin binding and transport for the biosynthesis of heme; ion transport and immunomodulation [24, 25]. Although the PBR is mainly located in the outer mitochondrial membrane, especially at the contact sites of the outer and inner mitochondrial membranes, it can be also found in nuclear fractions of normal and cancerous human liver tissue and in the plasma membrane and membrane of organelles in various cell types [26–29].

In the CNS, PBRs are mainly located in glial cells, particularly in microglia and astrocytes, with highest densities in the olfactory bulb, choroid plexus, and the ependymal lining of the ventricles [17, 30]. In the CNS, PBRs participate in multiple physiological functions including neurosteroid synthesis, nutritional support of neurons, and modulation of CNS immune reactions. The expression of the PBR in brain is significantly increased in response to a wide variety of CNS insults. Experimental results show that such increases are mainly due to activated glial cells. In response to intercellular signaling induced by neurotoxicants, microglial activation

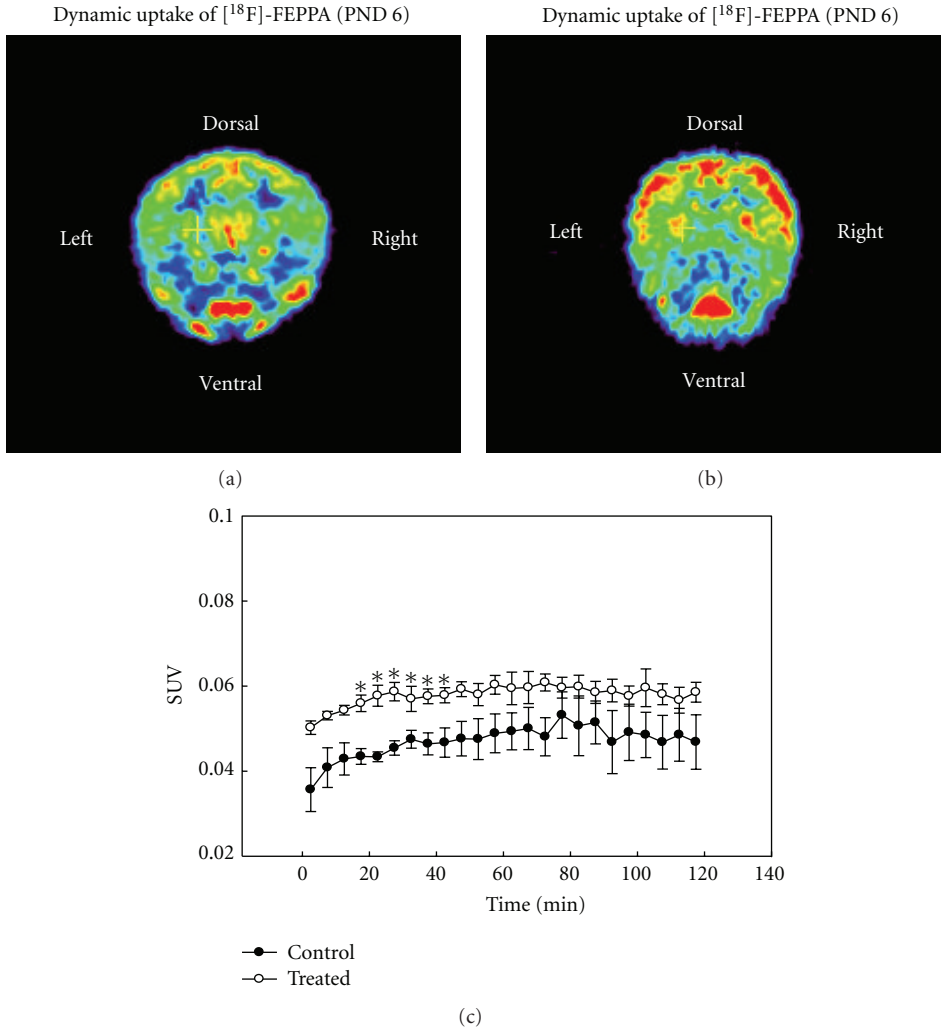

Figure 3: A set of representative microPET images (coronal plane) of a control (a) and a treated monkey brain (b) on PND 6. Graph (c) shows the dynamic uptake of [^{18}F]-FEPPA expressed as SUV versus time for each ROI (left temporal lobe) from control and anesthetic-treated monkeys on PND 6 or 7 (n = 4/group). SUV = standard uptake value = average concentration of radioactivity in the ROI (MBq/mL) $\times$ body weight in grams/injected dose (MBq). Data are shown as the means $\pm$ SEM $^*P < 0.05$.

usually begins several hours after exposure and lasts for several days after injury onset [31–33]. In their activated state, microglia undergo morphological changes, accumulate and proliferate at the site of neuronal damage, synthesize proinflammatory cytokines, and release toxic molecules and metabolites to eliminate damaged cells. Activation of microglia also may indicate that they are performing some protective functions such as releasing neurotrophic factors and protecting cells from damage [32, 34, 35]. Various studies have demonstrated that PBRs are involved in numerous nervous system disorders such as multiple sclerosis, cerebral ischemia and stroke, epilepsy, brain injury, neurotoxic brain damage, and neurodegenerative diseases [17, 34–37].

Following exposure to neurotoxicants and after other forms of neuronal insult, PBR levels increase significantly in both astrocytes and microglia in damaged brain areas in a time-dependent and region-specific fashion. After brain injury, immunolabelling of PBRs has been shown to increase with the increase being localized to mitochondria and other cellular compartments [17, 38, 39].

Molecular imaging using positron emission tomography (PET) is a minimally invasive approach for tracking biochemical and physiological processes in vivo. Astrogliosis, an abnormal increase in the number of astrocytes generally caused by the destruction of nearby neurons, is considered a universal marker of neurotoxicity/neurodegeneration. The PBR is widely recognized as an important target for PET imaging because PBR levels increase in areas of neuronal injury/neurotoxicity following insult. Several specific ligands for the PBR have been radiolabeled and used in in vivo studies in nonhuman primates. Among them, the [^{18}F]-radiolabelled phenoxyanilide, [^{18}F]-FEPPA can be efficiently prepared in high radiochemical yields, and at high specific activity. This compound has appropriate lipophilicity for

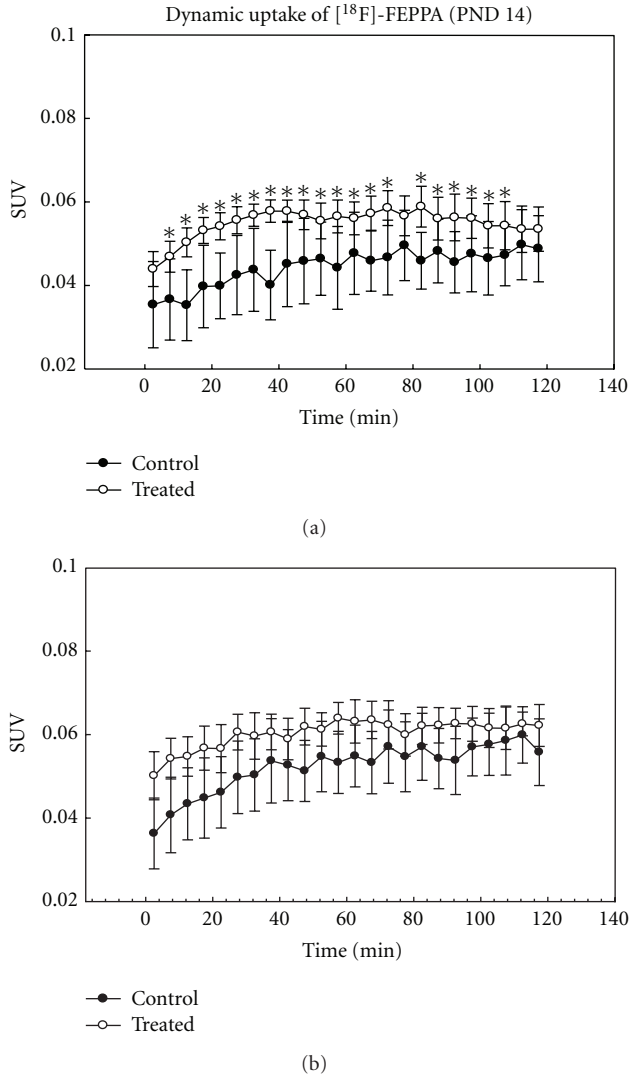

Figure 4: Graph showing the dynamic uptake of [^{18}F] -FEPPA expressed as SUV versus time in the ROI ((a) left frontal cortex; (b) left temporal lobe) from control and anesthetic-treated monkeys on PND 14 (n = 4/group). Data are shown as the means ± SEM $^*P <$ 0.05.

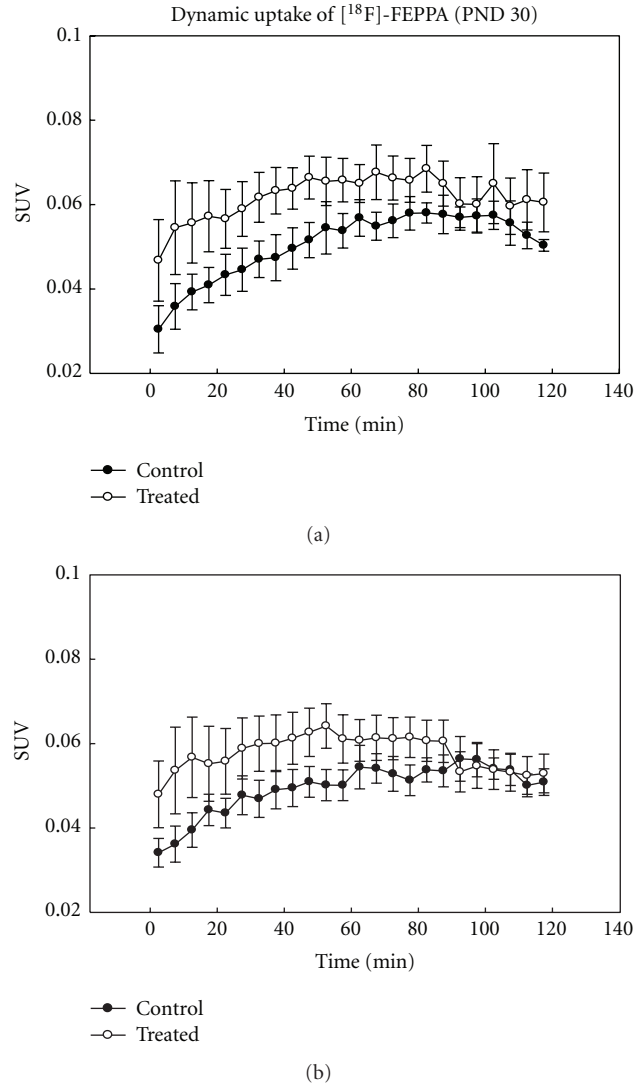

Figure 5: Graph showing the dynamic uptake of [^{18}F] -FEPPA expressed as SUV versus time in the ROIs ((a) left frontal cortex; (b) left temporal lobe) from control and treated monkeys on PND 30 (n = 4/group). Data are shown as the means ± SEM $^*P < 0.05$.

assisting brain penetration and has shown moderate uptake in the rat brain [19, 25, 40, 41].

One of the strengths of the present study is the use of the developing nonhuman primate as the experimental model. Data from rodent models have implicated some gaseous anesthetics as being toxic to the developing brain and some studies have reported cognitive deficits in later life after such exposures [4, 6]. However, there are no clinical data providing evidence that the pediatric use of these anesthetics is associated with signs of developmental neurotoxicity. Because of obvious limitations it is not possible to thoroughly explore the effects of pediatric anesthetic agents on neurons in human infants or children. It is also not feasible to determine the dose-response or time-course of potential anesthetic-induced neuronal cell death in human infants or children. Due to the complexity of the primate brain, the monkey is often the animal model of choice for neurotoxicological experiments, particularly in a developmental context. The monkey provides a closely-related animal model appropriate for examining the effects of pediatric anesthetics and other agents. The anatomical and functional complexity of the monkey CNS also facilitates the interpretation of data with respect to the extrapolation of findings to humans, and it is in the rhesus monkey that the phenomenon of interest (anesthetic-induced neuronal cell death) has been previously reported [21, 42].

Recent data from monkeys demonstrate cognitive deficits lasting years after a single prolonged exposure to the NMDA receptor antagonist ketamine [43]. The use of nonhuman primate models continues to garner considerable interest among anesthesiologists, pharmacologists, and toxicologists

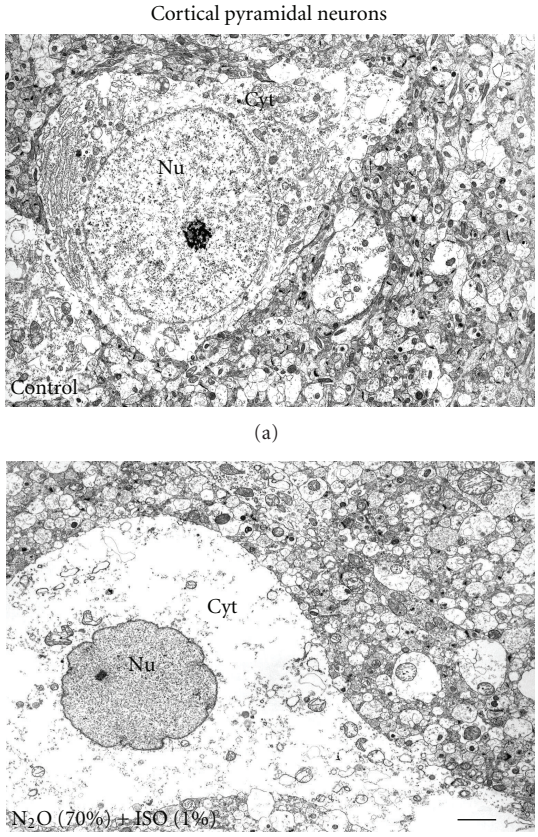

Figure 6: Electron micrograph (EM) showing a normal pyramidal neuron in the frontal cortex with intact cytoplasm and nuclear membrane from a control infant monkey (a). EM figure showing nuclear condensation (advanced state of apoptosis) and mitochondrial swelling and typical cell body swelling (necrosis) of pyramidal neurons (note nucleolus in the nucleus) in the frontal cortex (b) from a subject exposed to the inhaled anesthetic combination (N_2O + ISO) for 8 h. Nu = nucleus. Cyt = cytoplasm. Scale bar = 0.5 μm.

with growing recognition to be anticipated from surgeons and neonatologists. A host of mechanistic studies have been completed or are underway which are providing a rationale for the overall concern about anesthetic and sedative-induced neurotoxicity and teasing apart the causalities, refining hypotheses, and suggesting clinical strategies to test for and ameliorate the problem in patients. These have ranged from cell culture to histopathology to animal behavioral studies—including nonhuman primates [21, 43–45].

Shorter durations of anesthesia cause less or no cell death in monkeys: whether exposures to anesthetics will cause cell death in humans is still unknown, but it is most certainly likely that shorter exposure durations will have less impact than longer durations. Although drug combinations are commonly used in pediatric surgical procedures, there is a huge data gap on the neurodegenerative effects associated with anesthetic drug combinations. Therefore, it is essential to continue studies in monkeys to obtain important information on the time course and severity of observed effects. In a parallel morphological study [7], PND 5, or 6 rhesus monkeys were exposed to N_2O (70%) or ISO (1.0%) alone, or N_2O plus ISO for 3 or 8 h, respectively. Inhalation of the combination of 70% N_2O + 1% ISO produces a surgical plane of anesthesia. Six hours after completion of anesthetic administration the monkeys were examined for neurotoxic effects. No significant findings were observed in monkeys exposed to N_2O or ISO alone, or monkeys exposed to N_2O plus ISO for 3 h. However, enhanced neuronal damage was apparent when N_2O was combined with ISO for 8 hours: affected areas were seen in neocortical areas including the frontal cortex and in the temporal lobe. Consistent with the present microPET imaging findings, these data suggest that prolonged exposure to a combination of N_2O and ISO during early development results in neuronal damage in the rhesus monkey. Although [^{18}F]-FEPPA is not thought to directly label dying cells, it is thought to label PBRs and increases in their expression are thought to co-occur with adverse events such as neuronal damage and death. As such [^{18}F]-FEPPA, as a marker of gliosis, may be useful for indicating the location of neurons that are distressed. It is proposed that molecular imaging using this biomarker could help detect neurotoxicity in neonatal and infant rodents, monkeys, and humans alike. By repeatedly assessing the characteristics of the labeled FEPPA in affected areas [15, 16] it should be possible to evaluate the severity and time course of anesthetic-induced neural damage (e.g., apoptosis and/or necrosis). The use of the developing monkey would seem to provide an excellent bridging model to aid in the translation of findings in lower species to higher species, and thus, serve to provide the most expeditious approach toward decreasing the uncertainty in extrapolating pre-clinical data to the human condition.

Consistent with the microPET imaging data, direct evidence of enhanced neuronal damage after exposure to the inhaled anesthetic combination of N_2O and ISO was confirmed in treated monkey brain via electron microscopic analysis: neurons in the frontal cortex exhibited typical nuclear condensation and morphological changes including swelling of the mitochondria and cell bodies. These findings were observed at approximately the same age as the first microPET/CT scan was obtained and are characteristic of the advanced stages of apoptosis and necrosis. The EM approach was employed to better understand the nature of the inhaled anesthetic-induced neurotoxicity, not for quantitative analyses of the associated damage. The EM data indicate that inhaled anesthetic-induced neuronal cell death is both apoptotic and necrotic in nature in the developing rhesus monkey.

There is growing recognition that exposures to anesthetics and/or sedatives during very active periods of brain growth can cause neurotoxicity, notably in the form of apoptotic cell death in rodents and also necrosis in monkeys. Presently, causality is unclear but likely multifactorial. Genomic predisposition may be a factor. The apparent elevated PBR levels reported here suggest that increased microglial activation and astrocytosis accompanies anesthetic-induced neurotoxicity. Significant brain injury in both the temporal cortex at one day, and frontal cortex at

one week after anesthetic exposure was suggested by the time course of the FEPPA retention reported here. The reasons underlying the different time courses in these different brain areas are not known but seem to indicate differential sensitivities of different brain areas to anesthetic-induced neurotoxicity. It may also indicate that different populations of PBRs are activated at different times: microglial activation apparently lasts for several days after injury whereas astrocytosis is thought to peak around 10 days after toxic insult [32, 39].

The action of NMDA antagonists or GABA agonists is thought to increase overall nervous system excitability and contribute to abnormal neuronal cell death during development. It is increasingly apparent that mitochondria lie at the center of the cell death regulation process. Evidence for the role of oxidative stress in anesthetic-induced neurotoxicity has been generated in studies that have manipulated levels of oxidative stress. Thus, it will be important to determine whether injury to brain tissue caused by anesthetic and/or sedative exposure can be prevented or ameliorated by the coadministration of antioxidants. L-carnitine, an antioxidant dietary supplement, has been reported to prevent neuronal damage [46]. L-carnitine is also well known to modulate membrane integrity thereby preserving cellular function. In a parallel microPET study, the potential protective effects of L-carnitine on inhaled anesthetic-induced neuronal damage were examined in rats by monitoring changes in the uptake of [^{18}F]-FEPPA. Those experiments demonstrated that co-administration of L-carnitine (300 mg/kg) blocks the increase in [^{18}F]-FEPPA uptake induced by the N_2O plus ISO combination used in the present experiments (data not shown). Thus, there are likely ways in which the toxicity associated with exposures to anesthetics and/or sedatives can be blocked or at least greatly attenuated.

There are yet many questions that need to be answered before the findings of anesthetic-induced neurotoxicity observed in animals can be related to the clinical situation. However, the use of a nonhuman primate model combined with molecular imaging tools might be one of the most practical approaches for evaluating the location, the time course, and the severity of neuronal damage associated with anesthetic or sedative exposures during development.

In summary, this is the first paper on the application of microPET in an attempt to quantify the uptake of [^{18}F]-FEPPA in the nonhuman primate brain after neonatal exposure to a combination of nitrous oxide (70%) and isoflurane (1%). The imaging data presented here are thought to demonstrate the ability of microPET to quantitate a putative biomarker of neurotoxicity (the PBR) using the ^{18}-F-labeled PBR ligand, FEPPA. Should it be further demonstrated that the PBR is a useful marker of neurotoxicity/neurodegeneration, regardless of the exact mechanism, then the use of [^{18}F]-FEPPA and similar compounds should provide incredible opportunity for the minimally-invasive monitoring of the health of the brain in humans as well as animals.

Acknowledgments

This paper has been reviewed in accordance with United States Food and Drug Administration (FDA) policy and approved for publication. Approval does not signify that the contents necessarily reflect the position or opinions of the FDA nor does mention of trade names or commercial products constitute endorsement or recommendation for use. The findings and conclusions in this paper are those of the authors and do not necessarily represent the views of the FDA. This work was supported by the National Center for Toxicological Research (NCTR)/US Food and Drug Administration (FDA).

References

[1] L. L. Campbell, J. A. Tyson, E. E. Stackpole et al., "Assessment of general anaesthetic cytotoxicity in murine cortical neurones in dissociated culture," *Toxicology*, vol. 283, no. 1, pp. 1–7, 2011.

[2] M. D. Krasowski and N. L. Harrison, "General anaesthetic actions on ligand-gated ion channels," *Cellular and Molecular Life Sciences*, vol. 55, no. 10, pp. 1278–1303, 1999.

[3] C. Wang and W. Slikker Jr., "Strategies and experimental models for evaluating anesthetics: effects on the developing nervous system," *Anesthesia and Analgesia*, vol. 106, no. 6, pp. 1643–1658, 2008.

[4] V. Jevtovic-Todorovic, R. E. Hartman, Y. Izumi et al., "Early exposure to common anesthetic agents causes widespread neurodegeneration in the developing rat brain and persistent learning deficits," *Journal of Neuroscience*, vol. 23, no. 3, pp. 876–882, 2003.

[5] S. Wang, K. Peretich, Y. Zhao, G. Liang, Q. Meng, and H. Wei, "Anesthesia-induced neurodegeneration in fetal rat brains," *Pediatric Research*, vol. 66, no. 4, pp. 435–440, 2009.

[6] X. Zou, N. Sadovova, T. A. Patterson et al., "The effects of l-carnitine on the combination of, inhalation anesthetic-induced developmental, neuronal apoptosis in the rat frontal cortex," *Neuroscience*, vol. 151, no. 4, pp. 1053–1065, 2008.

[7] X. Zou, F. Liu, X. Zhang et al., "Inhalation anesthetic-induced neuronal damage in the developing rhesus monkey," *Neurotoxicology and Teratology*, vol. 33, no. 5, pp. 592–597, 2011.

[8] C. DiMaggio, L. S. Sun, A. Kakavouli, M. W. Byrne, and G. Li, "A retrospective cohort study of the association of anesthesia and hernia repair surgery with behavioral and developmental disorders in young children," *Journal of Neurosurgical Anesthesiology*, vol. 21, no. 4, pp. 286–291, 2009.

[9] G. K. Istaphanous and A. W. Loepke, "General anesthetics and the developing brain," *Current Opinion in Anaesthesiology*, vol. 22, no. 3, pp. 368–373, 2009.

[10] C. J. Kalkman, L. Peelen, K. G. Moons et al., "Behavior and development in children and age at the time of first anesthetic exposure," *Anesthesiology*, vol. 110, no. 4, pp. 805–812, 2009.

[11] R. T. Wilder, R. P. Flick, J. Sprung et al., "Early exposure to anesthesia and learning disabilities in a population-based birth cohort," *Anesthesiology*, vol. 110, no. 4, pp. 796–804, 2009.

[12] A. T. Hillmer, D. W. Wooten, J. Moirano et al., "Specific $\alpha 4\beta 2$ nicotinic acetylcholine receptor binding of [F-18]nifene in the rhesus monkey," *Synapse*, vol. 65, no. 12, pp. 1309–1318, 2011.

[13] M. R. Kilbourn, B. Hockley, L. Lee et al., "Positron emission tomography imaging of (2R,3R)-5-[^{18}F]fluoroethoxybenzovesamicol in rat and monkey brain: a radioligand for the vesicular acetylcholine transporter," *Nuclear Medicine and Biology*, vol. 36, no. 5, pp. 489–493, 2009.

[14] D. W. Wooten, J. D. Moraino, A. T. Hillmer et al., "In vivo kinetics of [F-18]MEFWAY: a comparison with [C-11]WAY100635 and [F-18]MPPF in the nonhuman primate," *Synapse*, vol. 65, no. 7, pp. 592–600, 2011.

[15] X. Zhang, M. G. Paule, G. D. Newport et al., "MicroPET imaging of ketamine-induced neuronal apoptosis with radiolabeled DFNSH," *Journal of Neural Transmission*, vol. 118, no. 2, pp. 203–211, 2011.

[16] X. Zhang, M. G. Paule, G. D. Newport et al., "A minimally invasive, translational biomarker of ketamine-induced neuronal death in rats: microPET imaging using ^{18}F-annexin V," *Toxicological Sciences*, vol. 111, no. 2, pp. 355–361, 2009.

[17] S. Lang, "The role of peripheral benzodiazepine receptors (PBRs) in CNS pathophysiology," *Current Medicinal Chemistry*, vol. 9, no. 15, pp. 1411–1415, 2002.

[18] M. K. Chen and T. R. Guilarte, "Imaging the peripheral benzodiazepine receptor response in central nervous system demyelination and remyelination," *Toxicological Sciences*, vol. 91, no. 2, pp. 532–539, 2006.

[19] A. A. Wilson, A. Garcia, J. Parkes et al., "Radiosynthesis and initial evaluation of [^{18}F]-FEPPA for PET imaging of peripheral benzodiazepine receptors," *Nuclear Medicine and Biology*, vol. 35, no. 3, pp. 305–314, 2008.

[20] C. E. Hotchkiss, C. Wang, and W. Slikker, "Effect of prolonged ketamine exposure on cardiovascular physiology in pregnant and infant rhesus monkeys (Macaca mulatta)," *Journal of the American Association for Laboratory Animal Science*, vol. 46, no. 6, pp. 21–28, 2007.

[21] W. Slikker, X. Zou, C. E. Hotchkiss et al., "Ketamine-induced neuronal cell death in the perinatal rhesus monkey," *Toxicological Sciences*, vol. 98, no. 1, pp. 145–158, 2007.

[22] M. S. Berridge, S. M. Apana, and J. M. Hersha, "Teflon radiolysis as the major source of carrier in fluorine-18," *Journal of Labelled Compounds and Radiopharmaceuticals*, vol. 52, no. 13, pp. 543–548, 2009.

[23] C. Braestrup, R. Albrechtsen, and R. F. Squires, "High densities of benzodiazepine receptors in human cortical areas," *Nature*, vol. 269, no. 5630, pp. 702–704, 1977.

[24] V. Papadopoulos, M. Baraldi, T. R. Guilarte et al., "Translocator protein (18 kDa): new nomenclature for the peripheral-type benzodiazepine receptor based on its structure and molecular function," *Trends in Pharmacological Sciences*, vol. 27, no. 8, pp. 402–409, 2006.

[25] P. J. Schweitzer, B. A. Fallon, J. J. Mann, and J. S. D. Kumar, "PET tracers for the peripheral benzodiazepine receptor and uses thereof," *Drug Discovery Today*, vol. 15, no. 21-22, pp. 933–942, 2010.

[26] M. Hardwick, D. Fertikh, M. Culty, H. Li, B. Vidic, and V. Papadopoulos, "Peripheral-type benzodiazepine receptor (PBR) in human breast cancer: correlation of breast cancer cell aggressive phenotype with PBR expression, nuclear localization, and PBR-mediated cell proliferation and nuclear transport of cholesterol," *Cancer Research*, vol. 59, no. 4, pp. 831–842, 1999.

[27] B. O. Oke, C. A. Suarez-Quian, J. Riond, P. Ferrara, and V. Papadopoulos, "Cell surface localization of the peripheral-type benzodiazepine receptor (PBR) in adrenal cortex," *Molecular and Cellular Endocrinology*, vol. 87, no. 1–3, pp. R1–R6, 1992.

[28] J. M. M. Olson, B. J. Ciliax, W. R. Mancini, and A. B. Young, "Presence of peripheral-type benzodiazepine binding sites on human erythrocyte membranes," *European Journal of Pharmacology*, vol. 152, no. 1-2, pp. 47–53, 1988.

[29] I. Venturini, M. L. Zeneroli, L. Corsi et al., "Up-regulation of peripheral benzodiazepine receptor system in hepatocellular carcinoma," *Life Sciences*, vol. 63, no. 14, pp. 1269–1280, 1998.

[30] M. Imaizumi, E. Briard, S. S. Zoghbi et al., "Brain and whole-body imaging in nonhuman primates of [11C]PBR28, a promising PET radioligand for peripheral benzodiazepine receptors," *NeuroImage*, vol. 39, no. 3, pp. 1289–1298, 2008.

[31] R. B. Banati, "Neuropathological imaging: in vivo detection of glial activation as a measure of disease and adaptive change in the brain," *British Medical Bulletin*, vol. 65, pp. 121–131, 2003.

[32] F. Ito, H. Toyama, G. Kudo et al., "Two activated stages of microglia and PET imaging of peripheral benzodiazepine receptors with [11C]PK11195 in rats," *Annals of Nuclear Medicine*, vol. 24, no. 3, pp. 163–169, 2010.

[33] A. Takeuchi, "Microglial NO induces delayed neuronal death following acute injury in the striatum," *European Journal of Neuroscience*, vol. 10, no. 5, pp. 1613–1620, 1998.

[34] E. Briard, S. S. Zoghbi, M. Imaizumi et al., "Synthesis and evaluation in monkey of two sensitive 11C-labeled aryloxyanilide ligands for imaging brain peripheral benzodiazepine receptors in vivo," *Journal of Medicinal Chemistry*, vol. 51, no. 1, pp. 17–30, 2008.

[35] V. Papadopoulos, L. Lecanu, R. C. Brown, Z. Han, and Z. X. Yao, "Peripheral-type benzodiazepine receptor in neurosteroid biosynthesis, neuropathology and neurological disorders," *Neuroscience*, vol. 138, no. 3, pp. 749–756, 2006.

[36] J. Benavides, D. Fage, C. Carter, and B. Scatton, "Peripheral type benzodiazepine binding sites are a sensitive indirect index of neuronal damage," *Brain Research*, vol. 421, no. 1-2, pp. 167–172, 1987.

[37] N. Oku, T. Kashiwagi, and J. Hatazawa, "Nuclear neuroimaging in acute and subacute ischemic stroke," *Annals of nuclear medicine*, vol. 24, no. 9, pp. 629–638, 2010.

[38] A. C. Kuhlmann and T. R. Guilarte, "Regional and temporal expression of the peripheral benzodiazepine receptor in MPTP neurotoxicity," *Toxicological Sciences*, vol. 48, no. 1, pp. 107–116, 1999.

[39] A. C. Kuhlmann and T. R. Guilarte, "Cellular and subcellular localization of peripheral benzodiazepine receptors after trimethyltin neurotoxicity," *Journal of Neurochemistry*, vol. 74, no. 4, pp. 1694–1704, 2000.

[40] I. Bennacef, C. Salinas, G. Horvath et al., "Comparison of [11C]PBR28 and [^{18}F]FEPPA as CNS peripheral benzodiazepine receptor PET ligands in the pig," *Journal of Nuclear Medicine*, vol. 49, p. 81, 2008.

[41] P. M. Rusjan, A. A. Wilson, P. M. Bloomfield et al., "Quantitation of translocator protein binding in human brain with the novel radioligand 18 F-FEPPA and positron emission tomography," *Journal of Cerebral Blood Flow and Metabolism*, vol. 31, no. 8, pp. 1807–1816, 2011.

[42] X. Zou, T. A. Patterson, R. L. Divine et al., "Prolonged exposure to ketamine increases neurodegeneration in the developing monkey brain," *International Journal of Developmental Neuroscience*, vol. 27, no. 7, pp. 727–731, 2009.

[43] M. G. Paule, M. Li, R. R. Allen et al., "Ketamine anesthesia during the first week of life can cause long-lasting cognitive deficits in rhesus monkeys," *Neurotoxicology and Teratology*, vol. 33, no. 2, pp. 220–230, 2011.

[44] Z. Xie and R. E. Tanzi, "Alzheimer's disease and post-operative cognitive dysfunction," *Experimental Gerontology*, vol. 41, no. 4, pp. 346–359, 2006.

[45] S. Rizzi, C. Ori, and V. Jevtovic-Todorovic, "Timing versus duration: determinants of anesthesia-induced developmental apoptosis in the young mammalian brain," *Annals of the New York Academy of Sciences*, vol. 1199, pp. 43–51, 2010.

[46] C. Wang, X. Zhang, F. Liu, M. G. Paule, and W. Slikker, "Anesthetic-induced oxidative stress and potential protection," *The Scientific World Journal*, vol. 10, pp. 1473–1482, 2010.